NETWORKS AND HETEROGENEOUS MEDIA
©American Institute of Mathematical Sciences
Volume **8**, Number **4**, December **2013**

doi:10.3934/nhm.2013.8.985

pp. **985–1007**

STRUCTURED FIRST ORDER CONSERVATION MODELS FOR PEDESTRIAN DYNAMICS

Dirk Hartmann and Isabella von Sivers

Siemens AG, Corporate Technology
80200 Munich, Germany

(Communicated by Benedetto Piccoli)

Abstract. In this contribution, we revisit multiple first order macroscopic modelling approaches to pedestrian flows and computationally compare the results with a microscopic approach to pedestrian dynamics. We find that widely used conservation schemes show significantly different results than microscopic models. Thus, we propose to adopt on a macroscopic level a structured continuum model. The approach basically relies on fundamental diagrams - the relationship between fluxes and local densities - as well as the explicit consideration of individual velocities, thus showing similarities to generalised kinetic models. The macroscopic model is outlined in detail and shows a significantly better agreement with microscopic pedestrian models. The increased realism, important for safety relevant real life applications, is underlined considering several scenarios.

1. **Introduction.** Simulation of pedestrian streams is an emerging topic in the early design phases of large buildings and infrastructure as well as the operation of these. Typical questions range from those concerning convenience to security concerns: Do people feel comfortable? Is the level of service adequate? What are typical egress / evacuation times? Can dangerous situations be prevented by actively routing pedestrian flows? In this contribution, we shall focus on regional evacuation as studied in the REPKA research project [41, 46]. Corresponding simulation studies involve the simulation of the same scenario with slightly modified initial conditions, parameters, or geometries. Thus computational models that are both efficient and realistic are required. In contrast to long studied traffic phenomena (for a review see e.g. [4]), pedestrian dynamics are relatively new and more complex, especially since pedestrians flows are usually not guided by lanes. For an overview of the topic we refer e.g. to [2, 4, 23, 31, 42, 48].

Pedestrian flows are studied from an empirical as well as theoretical point of view. From an empirical point of view, two important quantitative findings of pedestrian flows have been obtained in the past (c.f. Figure 1): On the one hand, pedestrian free flow velocities (the velocity a pedestrian takes if he can move freely) are not constant but rather stochastically distributed, typically a Gaussian distribution is assumed [51]. On the other hand, pedestrians adapt their velocity according to the local density [4, 48, 49, 51], i.e. they tend to move slower in denser crowds. The

2010 *Mathematics Subject Classification.* Primary: 35L65, 35Q91; Secondary: 90B10, 91D10.
Key words and phrases. Pedestrian flows, pedestrian dynamics, regional evacuation, macroscopic models, microscopic models, generalised kinetic theory, cellular automata, conservation equation, transport equation, hyperbolic models.

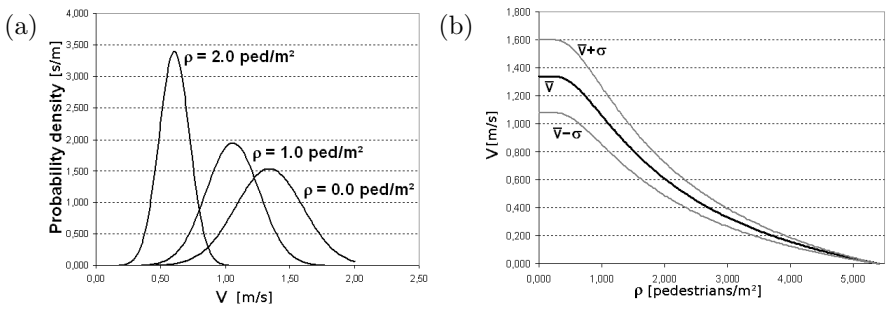

FIGURE 1. Distribution of pedestrian velocities according to [51]: (a) Free flow velocities v_{ff} of pedestrians are normally distributed ($\bar{v_{\text{ff}}} = 1.34$, $\sigma = 0.26$ in case of a local density of 0.0 ped./m^2) and (b) are adapted to the local density according to $v(\rho, v_{\text{ff}}) = v_{\text{ff}}(1 - \exp(-\gamma(1/\rho - 1/\rho_{\max})))$ where $\gamma = 1.913$ and $\rho_{\max} = 5.4$.

latter relationship between velocity and density is referred to as the fundamental diagram. The most popular is probably $v(\rho, v_{\text{ff}}) = v_{\text{ff}}(1 - \exp(-\gamma(1/\rho - 1/\rho_{\max})))$ given by [51] where γ is a parameter, $\rho_{\max}$ describes the maximum density which can be realised, and v_{ff} is the free flow velocity. Thus any model should at least reflect these two important empirical findings.

Conceptually, models of pedestrian flows can be distinguished between microscopic and macroscopic models (for a classification c.f. Figure 2) [2, 4, 23, 31, 42, 48]. Microscopic models consider single pedestrians and their behaviour whereas macroscopic models consider the evolution of pedestrian densities. Microscopic models are typically based on discrete cellular automaton descriptions [6, 7, 16, 19, 22, 33, 34, 40, 50, 54] or social force models [11, 14, 25, 37, 39, 43, 53]. The main advantage of microscopic models is the detailed resolution of single pedestrian's behaviour, which provides reliable results. At the same time this implies that these models are relatively complex from a computational point of view. Macroscopic models can usually be computed much more efficiently. Two popular approaches are PDE-based models [8, 12, 13, 20, 21, 28, 29, 30, 31, 52] in one or two dimensions which model densities instead of single pedestrians, or discrete network models [18, 27]. The latter are even more efficient to solve and thus are often used when facing large crowds or in optimisation frameworks. Furthermore, continuum models are very useful for determining general principles for which microscopic models, with their reliance on numerical methods, cannot be used. Although from a computational point of view these models are much more attractive, their validity (and thus reliability) is a priori not obvious, especially in extreme situations, and has to be proven in each scenario separately.

Recently [2, 4] have proposed to use generalised kinetic theories, well established in traffic models, for modelling pedestrian flows (c.f. also [20, 21]). In addition to the idea of using a generalised kinetic theory for pedestrian flows, several works adopting a multiscale perspective on pedestrian flows have been developed in the literature. For example, [35, 36] have used a discrete network flow optimisation approach to optimise egress times (using a constant velocity for all pedestrians independent of the local density) of a virtual evacuation of a soccer stadium and

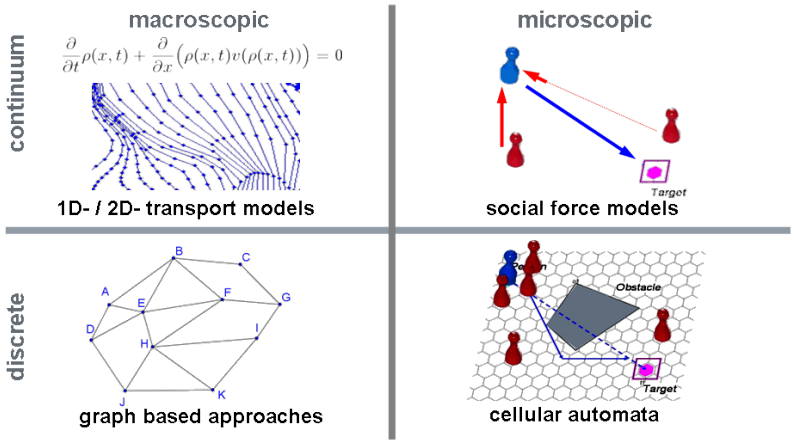

FIGURE 2. Schematic classification of pedestrian flow models

compared these results with a microscopic model using exactly the same egress strategy. Moreover, [12] has proposed a truly multiscale approach in the framework of transport equations and measure theory. The approach explicitly considers fundamental relationships between pedestrian velocities and local densities but does not explicitly account for different free flow velocities among individuals (as suggested by empirical findings).

Inspired by these works, we shall investigate the detailed relationship between well established microscopic models for pedestrian flows and classical macroscopic PDE-based models in more detail on a computational basis. In the following, we shall restrict ourselves to directed quasi one-dimensional flows (on networks), since our main emphasis is regional evacuation (c.f. Figure 3, [41, 46]). On the microscopic level, we shall rely on the well established cellular automaton model detailed in [19, 33]. However the findings should also hold for most other models. On the macroscopic level, we consider one-dimensional first order PDE-based models, where the velocity of pedestrians is given by a fundamental diagram. These are extended on networks following the approach of [10].

Our results show that the spatio-temporal dynamics between microscopic and macroscopic models agree quite well if the free-flow velocities in the microscopic model are constant among individuals. However, assuming a distribution of different free-flow velocities among individuals the spatio-temporal dynamics differ significantly. Thus, we propose an extension of macroscopic transport models to explicitly include differences in free-flow velocities among individuals. To do so, we introduce an additional structure as suggested by a generalised kinetic theory [2, 4] (c.f. also [20, 21]). When considering such structured transport models for pedestrian flows a perfect agreement with detailed microscopic models is found on a computational basis. Although the structured transport models are slightly more complex from a computational point of view the increased reliability cannot be overestimated with respect to real world applications.

The new contributions of our work are:

- systematic computational comparison of microscopic and macroscopic models,

FIGURE 3. Snapshot of a microscopic simulation - regional evacuation of 40 000 pedestrians leaving the Fritz-Walter soccer stadium in Kaiserslautern, investigated in the REPKA project [41, 46]. Single pedestrians are marked by dots coloured according to the local density.

- realisation of a structured macroscopic model for pedestrian flows capturing dynamics and egress times significantly more realistic than classical macroscopic models,
- detailed computational studies investigating the proposed model.

Furthermore, we outline in the Appendix an alternative microscopic discrete-in-time model for pedestrian flows, which is as realistic as the proposed structured macroscopic model and as efficient from a computational point of view.

The article is structured as follows: we shall shortly review first order classical macroscopic models (where the velocity-density relation is determined via a fundamental diagram) as well as the microscopic model of [19, 33] and compare both types of models by computational means in Section 2. In the next step, an extension of the macroscopic models to include an additional structure will be introduced (Section 3). The extended model is investigated by computational means and shows a significantly better match with microscopic models than classical models. In Section 4, two more complex examples are investigated showing the advantages of the new approach. The article closes with a conclusion in Section 5. An interpretation of the proposed approach in terms of time-evolving measures, the applied numerical schemes, as well as an alternative discrete macroscopic multiscale approach are outlined in the Appendix.

2. Classical microscopic and macroscopic models.

2.1. Continuous macroscopic models.

The most fundamental property of pedestrian flows is the balance of pedestrians. Adopting a one-dimensional continuum point of view, i.e. considering pedestrian densities ρ rather than single pedestrians, it thus holds in the most general case:

$$\frac{\partial \rho(x,t)}{\partial t} + \frac{\partial}{\partial x}\left(v\left(\rho(x,t);x,t\right)\rho(x,t)\right) = f(x,t) \qquad \text{in } \Omega \times [0,T[\tag{1}$$

where $v(\rho(x,t);x,t)$ is the velocity of the pedestrians, $f(x,t)$ models origins or destinations of pedestrians, i.e. sources or sinks of pedestrians, and $\Omega \subset \mathbb{R}$ is the domain of interest. Here, we restrict ourselves to a one-dimensional approach but a generalisation to two dimensions is straightforward. Within this work, we consider the case $f(x,t) = 0$ and realize sources and sinks of pedestrians via boundary conditions. Thus the balance equation (1) models the conservation of pedestrians. Furthermore, we restrict ourselves to first order models [8] in the following, i.e. models where the closure between velocity and density is obtained by an explicit formula $v(\rho;x,t)$ - the fundamental diagram. For higher order models, introducing additional evolution equations for pedestrian velocities, we refer e.g. to the review [4]. Although this restriction reduces the explanatory character of the model, we believe that with respect to real world applications such a first order closure approach is more reliable. Experimental relationships are available [4, 48, 49, 51] and more complex models are non trivial to parametrise. The balance equation (1) is a classical equation in continuum mechanics with a long history in mathematical research [38]. Although within this work we concentrate on pedestrian flows [2, 4, 8, 12, 13, 20, 21, 28, 29, 30, 31, 42, 52], most of the aspects also hold for traffic flows [4, 5] being very similar to pedestrian flows.

In this contribution, we shall restrict ourselves to directional flows on quasi one-dimensional networks of streets. Considering regional evacuations [41, 46] this approach is clearly valid since streets are typically significantly longer than wide (c.f. Figure 3). For simplicity, we shall concentrate first (in this Section as well as in Section 3) on single streets to compare the different models - as it is suggested in the majority of works considering PDE-based approaches [18]. In Section 4, we shall then consider networks of streets. To map PDEs on networks, it is necessary to define coupling conditions at nodes ensuring the balance of mass [18]. For instance, this is done in traffic flow [3, 10, 24, 26] or supply chain modelling [17]. Here we shall follow the approach of [13] maximising the gross flux at each node according to a given distribution function while continuity of fluxes is ensured, i.e. pedestrians are conserved.

This classical model (2) is based on a description in terms of continuous scalar fields, i.e. densities. However an interpretation in terms of measure theory is possible, c.f. [12] or Appendix A.

Macroscopic models with constant velocities. The balance equation (1) has been considered in many works dealing with pedestrian flows. The simplest assumption would be that all pedestrians move with the same constant velocity v [31]. Adopting this assumption, equation (1) reduces to

$$\frac{\partial \rho(x,t)}{\partial t} + v\frac{\partial}{\partial x}\rho(x,t) = f(x,t) \qquad \text{in } \Omega \times [0,T[, \tag{2}$$

i.e. a simple transport equation. In a recent work by [18], it has been shown that under certain conditions the transport equation (1) coincides with discrete network flow models - a classical approach to optimizing pedestrian dynamics.

Macroscopic models with density dependent velocities. Although models based on the formulation (2) with constant pedestrian velocities are sometimes used, their validity is questionable. According to empirical results, e.g. [49, 51], the assumption of a constant velocity for all pedestrians does not hold in general. Following e.g. [51], the velocity of pedestrian flows depends on the local pedestrian density according

to

$$v(v_{\mathrm{ff}}, \rho; x, t) = v(v_{\mathrm{ff}}, \rho) = v_{\mathrm{ff}} \left(1 - \exp^{\left(-\gamma\left(\frac{1}{\rho} - \frac{1}{\rho_{\max}}\right)\right)}\right) \tag{3}$$

where γ is a parameter, $\rho_{\max}$ describes the maximum density which can be realised and v_{ff} is the so called free flow velocity. A classical choice for average European pedestrian flows is $\gamma = 1.913$, $v_{\mathrm{ff}} = 1.34$ and $\rho_{\max} = 5.4$ [51]. Although the exact form of the fundamental diagram is under discussion in the community of pedestrian flow experts and might even change from scenario to scenario, the existence of such a relationship is a fundamental aspect in pedestrian flows [4, 48, 49, 51] as well as in traffic flows [4, 15, 32, 44]. Thus most models, e.g. [8, 12, 13, 28, 29, 30, 52], explicitly include the fundamental diagram, i.e. rely on the balance equation (1) with the velocity v given by a fundamental diagram, e.g. the relationship (3) determined by Weidmann [51].

2.2. **Discrete microscopic models.** Most microscopic simulators share a common modelling approach of pedestrian behaviour. The different influences on each pedestrian, e.g. repulsion from other pedestrians, are modelled via forces (respectively potentials), i.e. models are inspired by simple Newtonian mechanics. Since many approaches rely on conservative potentials, forces and potentials based descriptions can be considered to be somewhat "equivalent".

To be more precise, we consider in the following the efficient microscopic pedestrian simulator introduced in [19, 33]. The approach is based on a cellular automaton using a hexagonal grid. At each time step every cell has a certain state: It is either empty or occupied by a pedestrian or a fixed obstacle. Following [51] pedestrians move with individual velocities depending on the local density (velocities are not discretised thus that in average "arbitrary" velocities can be realised). That is, to each individual pedestrian p a constant free flow velocity v_{ff}^p, which does not change in time, is assigned. The velocities v_{ff}^p are chosen according to a Gaussian distribution as postulated by [51]. The actual velocity of the pedestrian v^p is then chosen according to (3) where the density ρ is determined by local sampling and averaging within a radius R. It has been verified using the test case 4 of the RIMEA consortium [47] that different sampling strategies with different sampling radii do not affect the simulation results significantly.

The update scheme of the cellular automaton has to guarantee that pedestrians with higher velocities are allowed to move more often than pedestrians with lower velocities. In each time step of the simulation it is decided in a probabilistic fashion which set of pedestrians is allowed to move: faster persons are chosen more often such that, on average, pedestrians move with their prescribed velocity. The model's update rules are based on a potential description. Pedestrians are attracted by targets modelled as long-range potentials [19] and they repel each other by a force modelled through short-range potentials. In the simplest case, the movement rule for a single pedestrian is purely deterministic: move to the unoccupied neighbouring cell with the minimal total potential value. In general, the approach uses more complex rules (c.f. [19, 33]) to reduce discretisation artefacts to a minimum.

The model is quite similar to the so-called static floor field cellular automaton (cf. [7] and further references in [48]). However, compared with classical cellular automaton models artefacts originating from spatial discretisations of the cellular automaton lattice are reduced to a minimum by introducing appropriate corrections within movement strategies [19, 33]. Still the computational efficiency is not

affected. The resulting movement can hardly be distinguished from continuum approaches that typically require significantly more computational effort. It reliably captures typical crowd phenomena and could simulate up to 50 000 pedestrians, as required for typical regional evacuation settings [41, 46]. A typical simulation of a regional evacuation with 40 000 pedestrians in nearly real-time using the outlined cellular automaton approach is shown in Figure 3. For more details on the approach we refer to the original papers [19, 33].

2.3. **Comparison of microscopic and macroscopic models.** Let us now compare the different modelling approaches introduced above, namely macroscopic density based models (Section 2.1) as well as the microscopic model (Section 2.2). Since a rigorous mathematical treatment seems to be feasible only for relative simple cases, e.g. [18], we shall compare the different models by computational means considering a one-dimensional representation of a street with constant width. (We would like to stress that the continuum models can often also be solved analytically, e.g. using conformal mapping [28]). For completeness, we outline the first order finite volume scheme used to discretise the macroscopic models of Section 2.1 in Appendix B. The scheme differs from conventional upwind schemes to ensure important properties of pedestrian flows, i.e. the existence of a maximum density. The computational approach to microscopic models is more or less evident from the outline in Section 2.2, for more details we refer to the original papers [19, 33].

In the following, let us consider a long street of length $l = 200$m and width $w = 10$m for simplicity. Since $w/l \ll 1$, a one-dimensional approximation is valid. Furthermore, we assume that people are standing together in a square pedestrian block (10 m x 10 m) at the beginning of the street and move to the right during the course of the simulation. Here, we restrict ourselves to one way pedestrian flows as expected in a regional evacuation, but concepts for generalisations can be found in the literature, e.g. [1].

A natural metric for comparing different pedestrian flow models are evacuation times (one of the most common functional of interest). However, in a typical microscopic model predictions can be obtained only in a statistical sense [34]. Microscopic models include at least some randomness, such that the evacuation time depends on the detailed realisation. Therefore, the evacuation time of 90% (or a different proportion) of the pedestrians in the scenario is a better functional for the purposes of comparing different approaches. This ensures that arbitrary slow pedestrians which are likely to occur within the Gaussian distribution of free flow velocities are neglected by the functional of interest. In the following, we shall furthermore consider another metric for comparison which reflects information on the actual dynamics better than evacuation times: namely snapshots of densities at different time steps.

Balance equation vs. microscopic model with constant velocities. Let us consider the transport equation (2) and the microscopic model outlined in Section 2.2 along with the assumption that in the microscopic model all pedestrians p are walking with the same velocity, i.e. $v^p = 1.34$ m/s. The results are shown in Figure 4. We find that both approaches agree reasonably. Bearing in mind the accuracy of being able to model real pedestrian behaviour at all, the agreement of the two types is quite exact (at least from our point of view).

Balance equation vs. microscopic model using a fundamental relation. However, following the observation of Weidmann the assumption of a constant velocity v^p is

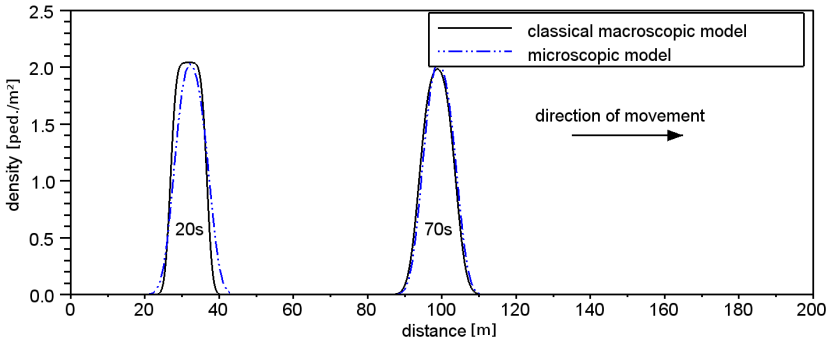

FIGURE 4. Comparison of an individual based microscopic models and density based macroscopic model (using a finite volume scheme with $\Delta_x = 0.1$m for simulations) for pedestrian flows moving from the left to the right in a street (length = 200m, width = 10m, persons = 200). It is assumed that all pedestrians move with a constant velocity $v = 1.34$ m/s. Snapshots at two different time-steps are shown (20s and 70s).

not valid in general situations. In a second step, we therefore compare simulations of the microscopic model with a behaviour mimicking Weidmann's relationship, i.e. v^p is given by relation (3) with constant $v_{\text{ff}}^p = 1.34m/s$ and ρ determined via local sampling and averaging (c.f. Section 2.2), and the macroscopic balance equation (1) with the relation (3) as well as the same v_{ff} for all pedestrians, i.e. variations among individuals are neglected. Results are shown in Figure 5. Again the simulations agree reasonably with respect to the expected accuracy. Bumps in the microscopic model are due to binning and the grid resolution of the microscopic model. They depend on the detailed binning and discretisation chosen.

Balance equation vs. microscopic model with distributed velocities. The continuum model considered in Figure 5 is a state-of-the-art model adopting a continuum macroscopic point of view [2, 4, 8, 31]. However, the microscopic model considered in Figure 5 does not include velocity variations among individuals, e.g. pedestrians of different sizes, ages or mobility, as state-of-the-art microscopic models do (c.f. e.g [48]). The variation of individual velocities is a fundamental and empirically well established property. Thus, we further compare the balance model (1) with a microscopic model reflecting variations of velocity among individuals as well as adapting velocities of pedestrians according to the local density, i.e. the velocity of a pedestrian v^p is given by (3) with v_{ff}^p given by a Gaussian distribution and ρ determined by local sampling and averaging (c.f. Section 2.2). Again, we chose the same setup as above. The results are shown in Figure 6. One can clearly observe that the macroscopic continuum model and the microscopic individual based model show a different qualitative behaviour - at least on the length scales regional evacuation is interested in.

Since the reliability of prediction of evacuation simulations depends on the realism of the simulation approaches [41], it is thus questionable whether typical macroscopic models outlined in Section 2.1 could be used instead of more realistic microscopic models. Thus an open question is whether there exists some type of

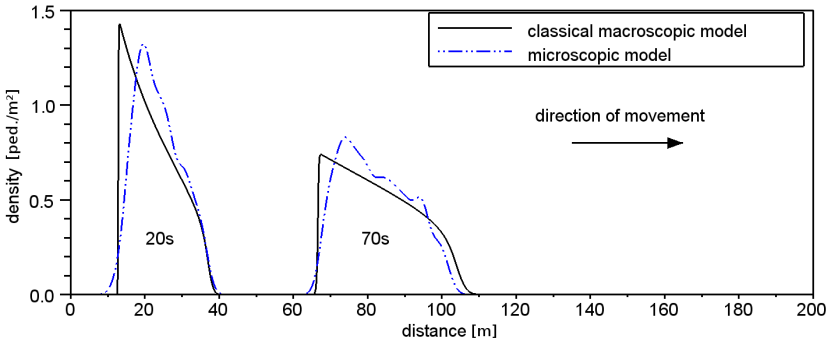

FIGURE 5. Comparison of an individual based microscopic model and density based macroscopic model (using a finite volume scheme with $\Delta_x = 0.1$m for simulations) for a pedestrian flow in a street (length = 200m, width = 10m, persons = 200) moving from the left to the right. It is assumed that all pedestrians move with a velocity according to Weidmanns fundamental relation (3) with the same $v_{\text{ff}} = 1.34$m/s for all pedestrians. Snapshots at two different time-steps are shown (20s and 70s).

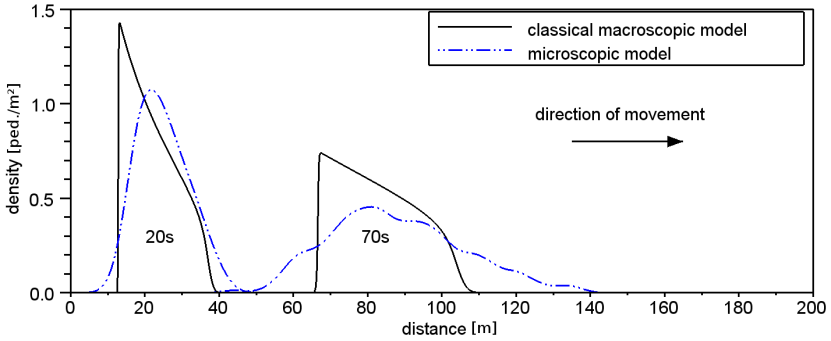

FIGURE 6. Comparison of an individual based microscopic and density based macroscopic model for a pedestrian flow in a street (length = 200m, width = 10m, persons = 200) assuming that all pedestrians move with a velocity according to Weidmanns fundamental relation (3) with $v_{\text{ff}} = 1.34m/s$, $\gamma = 1.913$ and $\rho_{\max} = 5.4\text{Ped}/m^2$. Snapshots at two different time-steps are shown (20s and 70s). The macroscopic model uses a spatial discretisation of $\Delta_x = 0.1$m.

macroscopic model that better mimics the behaviour of the microscopic model, i.e. realism. Finding an appropriate model is a rewarding task, for those interested in regional evacuation. However, computational efficiency is a crucial factor.

3. **Structured macroscopic transport model.** The drawback of the balance model (1) with the velocity given by relation (3) is the assumption that all pedestrians at a given point x and time t move with the same velocity $v = v(\rho(x,t))$. However, in general the velocities of the pedestrians differ among individuals. To increase the realism of current macroscopic models we therefore propose to include an additional structure - similar to generalised kinetic concepts recently suggested for pedestrian flows [2, 4] (c.f. also [20, 21]).

Therefore, we introduce in the following the additional variable v_{ff} modelling different free flow velocities among pedestrians in model (1). Thus, we consider densities ρ depending on space, time as well as the free velocity of individuals, i.e. $\rho(v_{\text{ff}}; x, t)$ is the density of pedestrians with free flow velocity v_{ff} at position x at time t. Hence, the total density of pedestrians at a point x at time t is given by

$$\rho(x,t) = \int_0^{v_{\text{ff}}^{\max}} \rho(\nu; x, t) d\nu, \tag{4}$$

where $v_{\text{ff}}^{\max}$ is the maximum free flow velocity any pedestrian can have. The free flow velocity is an individual property of pedestrians, i.e. a macroscopic state variable attached to each individual which does not change with time (not to be confused with the actual velocity used in kinetic models). Thus for modelling pedestrian flows the following balance equation holds

$$\frac{\partial \rho(v_{\text{ff}}; x, t)}{\partial t} + \frac{\partial}{\partial x}\left(v\left(v_{\text{ff}}; \rho(x,t)\right) \rho(v_{\text{ff}}; x, t)\right) = f(v_{\text{ff}}; x, t) \tag{5}$$

in $[0, v_{\text{ff}}^{\max}] \times \Omega \times [0, T[$, where $\rho(x,t)$ is given by (4). That is, (5) is an integro-differential equation and fundamental relation (3) is adapted accordingly, i.e. $v(v_{\text{ff}}; \rho) = v_{\text{ff}}(1 - \exp(-\gamma(1/\rho - 1/\rho_{\max})))$. Furthermore, $f(v_{\text{ff}}; x, t)$ models a source respectively sink term. An interpretation of the model in terms of time-evolving measures is given in Appendix A.

In the case of a single free flow velocity among individuals, model (5) reduces to the classical balance model (1), c.f. Appendix A. As in Section 2.1, we rely here on a first order closure, i.e. use experimental relationships for the velocity depending on the density rather than providing an additional model.

Structured macroscopic model vs. microscopic model. Considering the same setup as in Section 2.3, the structured balance equation (5) modelling pedestrian flows on a macroscopic level is compared with the microscopic model of Section 2.2 by computational means. To do so, we adopt a piecewise constant approximation with respect to v_{ff}. This corresponds to the introduction of different velocity classes of pedestrians (c.f. also [20]), each evolving according to equation (5), i.e. a system of n equations. For more details on the discretisation of the free flow velocity state we refer to Appendix A. The evolution of each velocity class is computed using the finite volume scheme outlined in Appendix B.

In Figure 7, the comparison of the structured macroscopic model with the detailed microscopic model using the same setup as in Section 2.3 is shown. One can clearly observe that both models agree quite well. Comparing this model with the macroscopic models outlined in Section 2.1, we find that the structured macroscopic model is expected to yield the most realistic results (c.f. Figure 8).

At the same time the structured macroscopic model is still relatively efficient from a computational point of view. To compare the different methods, the computation times for three different scenarios - streets of lengths 200m, 400m and 600m -

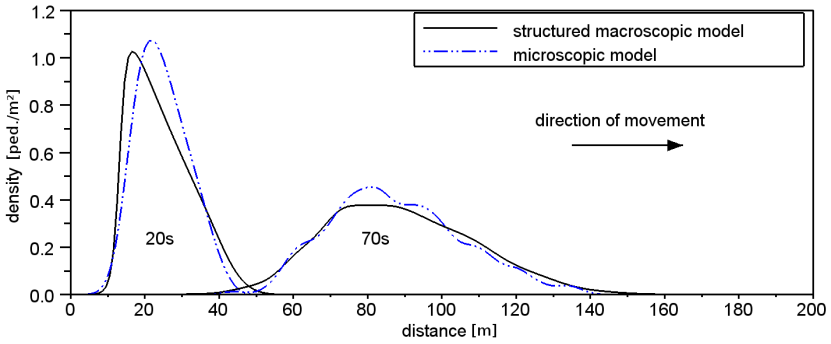

FIGURE 7. Comparison of an individual based microscopic and density based structured macroscopic model for a pedestrian flow in a street (length = 200m, width = 10m, persons = 200). Snapshots at two different time-steps are shown. The macroscopic model uses a spatial discretisation of $\Delta_x = 1$m and uses 10 velocity classes for a discretisation of the velocities.

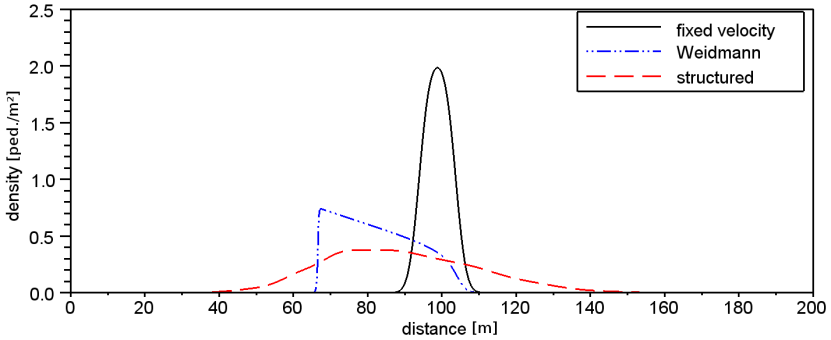

FIGURE 8. Comparison of different microscopic models simulating pedestrian flows in a street (c.f. Figures 4, 5,7). A snapshot at time 70 s is shown.

are compared in Table 1. 2000 pedestrians move from the left hand side to the right hand side of the street and the simulation stops when 50% of the pedestrians have left the street. Since the predicted evacuation time $t_{\text{evacuation}}$, i.e. the time it takes for 50% of the pedestrians to be evacuated, depends on the considered model, we believe that relative computation times $t_{\text{relative}} = t_{\text{computation}}/t_{\text{evacuation}}$ are an appropriate measure for computational efficiency. Here $t_{\text{computation}}$ is the time which has been spent on computations by the processor. Furthermore, we compare different discretisations of the macroscopic models (Δ_x =1m, Δ_x =10m). Additionally, the computational efficiency depends on the number of pedestrians considered. The microscopic model has roughly a linear dependence of relative computational times on the number of considered pedestrians, whereas the macroscopic models should not depend significantly on the number of pedestrians since they consider continuous densities. However, the evacuation time depends in both cases on the number

2000 persons	200m	400m	600m
Microscopic Model	0.049	0.044	0.047
Classical Macroscopic Model $\Delta x = 1m$	0.002	0.008	0.020
Classical Macroscopic Model $\Delta x = 10m$	0.00006	0.00009	0.0002
Structured Macroscopic Model $\Delta x = 1m$	0.007	0.039	0.082
Structured Macroscopic Model $\Delta x = 10m$	0.0002	0.002	0.002

TABLE 1. Computational efficiency of the microscopic, classical macroscopic and structured macroscopic model for pedestrian flows. Streets of three different length are considered and the computation is stopped after 50% of the pedestrians have left the street. The computational efficiency is measured in terms of relative computational times, i.e. $t_{\text{relative}} = t_{\text{computation}}/t_{\text{evacuation}}$.

of pedestrians since higher densities typically imply slower velocities according to the fundamental diagrams.

4. **Examples.** Let us now investigate the newly introduced structured macroscopic model in more detail considering two test cases: a narrowing street (Section 4.1) and a simple egress scenario, i.e. a network of one-dimensional streets (Section 4.2).

4.1. **Narrowing street.** So far, we have considered only streets of constant width, but frequently real scenarios include streets with narrowing passages causing congestions. Here we consider such an example. We assume a street of length 200m which has a width of 10m for the first 100m and a width of 4m for the rest of the street. 200 persons are moving from the left to the right. The street is split up into two parts of constant width and both parts are coupled according to [13] (c.f. also Section 2.1). Having only one incoming and one outgoing edge, the coupling conditions corresponds to a continuity of fluxes, i.e. $\int_{0\text{m}}^{10\text{m}} v^- \rho^- dy = \int_{0\text{m}}^{4\text{m}} v^+ \rho^+ dy$, where $^\pm$ indicate limits from the left hand and right hand sides respectively. A comparison of the classical macroscopic model using the fundamental diagram (3), the newly introduced structured model as well as the microscopic model is shown in Figure 9. Snapshots of densities at different time steps show a good agreement between the newly introduced structured macroscopic model and the microscopic models, whereas the comparison of the classical macroscopic model and the microscopic model shows significant qualitative differences.

4.2. **A simple egress scenario.** Before building or operating public infrastructure, typically detailed evacuation studies have to be performed to ensure minimum evacuation times - often legally required. Here, we consider a regional evacuation scenario. Given a scenario with an egress strategy the macroscopic models can be used to predict evacuation times. Furthermore, using optimisation algorithms in combination with efficient macroscopic simulation techniques corresponding optimal egress strategies can be developed. Such strategies are in many situations not obvious. Most pedestrians have multiple egress routes they could choose from. Furthermore, congestions might occur leading to highly non-linear relationships between the travelled distance and the required time [51].

In this section we shall investigate the small fictitious evacuation scenario shown in Figure 10 build up by a network of streets. Edges of the network are discretised as before and at the nodes we follow the approach of [10] prescribing explicitly the

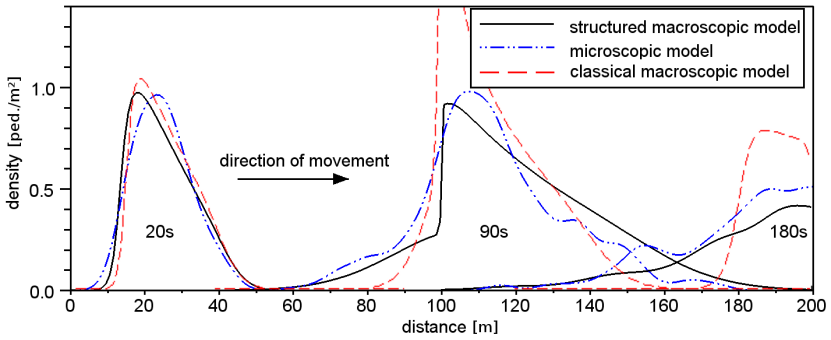

FIGURE 9. Comparison of a structured macroscopic model (using a finite volume scheme with $\Delta_x = 1$m for simulations) and an individual based microscopic model for a pedestrian flow in a narrowing street (length = 200m, width = [10m for the first 100m, 4m for the second 100m], persons = 200) moving from the left to the right. Snapshot at three different time steps of the simulation time are shown (20s, 90s, 180s).

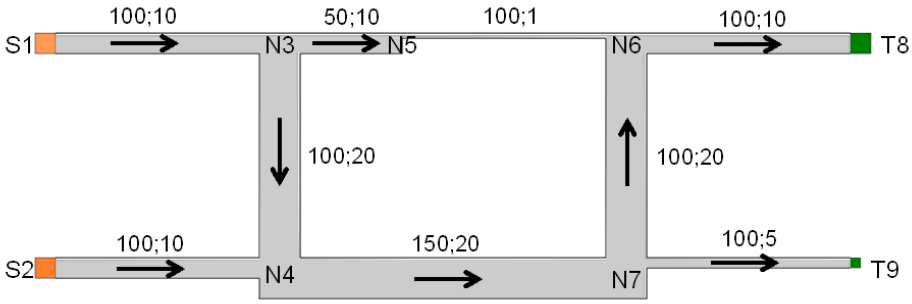

FIGURE 10. Fictive scenario with two sources (S1, S2) with 2000 persons per source (4000 total) entering the scenario as fast as possible. At the two targets (T8, T9) the persons leave the scenario. For the microscopic model the scenario is considered as a two-dimensional arrangement of streets, for the macroscopic model it is a graph with nodes (S1, S2, N3, ..., N7, T8, T9). The dimensions of the streets are shown above.

distribution of pedestrians (c.f. Section 2.1). At two sources with 2000 persons per source (4000 total) pedestrians enter the scenario as fast as possible on the left hand side. They try to leave the scenario at the two exits on the right hand side. Because of narrowing of streets an optimal evacuation strategy is not obvious. As a first guess pedestrians are routed according to street widths. That is, at the crossing N3 $33.\bar{3}\%$ of the pedestrians are routed to the vertex N5 and $66.\bar{6}\%$ to the vertex N4. Similarly at the vertex N7 80.0% are routed to N6 and 20.0% to T9. This routing strategy corresponds to an evacuation of 80% of the pedestrians in 647 seconds (c.f. also Table 2). Again, we consider not the full evacuation since

	Initial Distributions	Optimised Distributions
N3 → N4	$0.666\bar{6}$	0.8316
N3 → N5	$0.333\bar{3}$	0.1684
N7 → N6	0.800	0.5667
N7 → T9	0.200	0.4333
80% evacuation time	647 s	584 s

TABLE 2. Routing of pedestrians at nodes N3 and N7 in the fictive scenario shown in Figure 10. The initial routing of pedestrians according to width is not optimal as underlined by the optimised distribution.

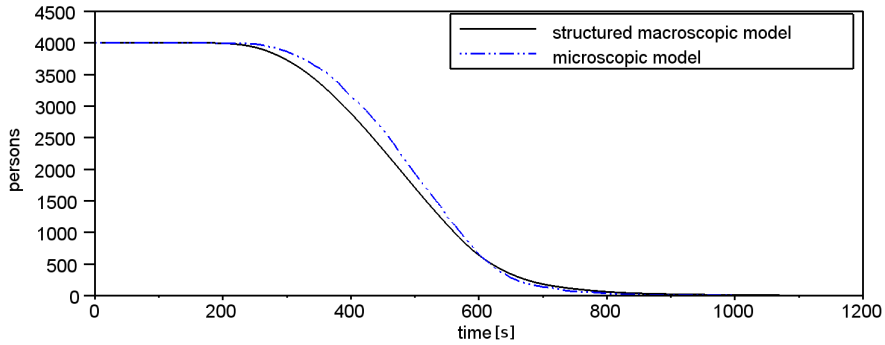

FIGURE 11. Population of our fictive evacuation scenario. Comparison of the structured macroscopic model and the microscopic model.

Gaussian distributions allow arbitrarily slow pedestrians, although in the structured macroscopic approach the discretisation of velocities defines of course a lower bound.

Because of the highly non-linear relationship of pedestrian velocities and densities, it is likely that this is not an optimal egress strategy. Therefore, we use in the following an optimisation approach to determine an optimal egress strategy. Here, we use the Nelder Mead method [45] but other methods work as well. The functional of interest is again the evacuation time when 80% of the pedestrians have left the scenario, i.e. an egress strategy is optimal if this time is minimal. Using the structured model an optimised egress strategy (c.f. Table 2) yields an egress time of 584 seconds, i.e. the egress time is improved by 10% compared with our naive strategy proposed above. Of course this might eventually be only a local minimum, although we have checked various other strategies to start the optimisation with, i.e. various starting points of the optimisation.

Using the same egress strategy for the microscopic model, we compare both approaches. The results are presented in Figure 11 and show a good agreement. Especially at the tail a good agreement is important since this is the critical region with respect to egress.

5. **Conclusions.** In this article, we have introduced a new PDE-model for the macroscopic description of pedestrian flows. This new macroscopic model is motivated by a computational comparison of classical macroscopic models and a microscopic model resolving single pedestrian behaviour. Comparing the dynamics, e.g. snapshots of density distributions at certain time steps, shows a significant difference between the microscopic model and classical macroscopic models.

In comparison to classical models the proposed macroscopic model introduces an additional structure, namely individual velocities of pedestrians (similar to generalised kinetic theories). Velocities are again adapted to the local density according to given fundamental diagrams. Thus the empirically observed distributions of individual free-flow velocities among pedestrians is resolved by the model. Dynamics of this improved model show nearly a perfect agreement with a detailed microscopic model, on single quasi-one-dimensional streets as well as on networks of streets.

The improved realism is extremely important for safety-relevant real life applications [41] - we are mainly concerned with regional evacuation [46]. The validation of egress strategies or identification of optimisation potentials depends critically on the reliability of the considered models. Thus, the realism in combination with the computational efficiency makes the developed macroscopic approach an ideal computational tool for the investigation of regional evacuation.

So far, we have considered only directed flows in one dimension, which is a reasonable assumption when studying regional evacuation. The extension of classical models to two-way flows in one dimension has been suggested by [1] and can be adopted accordingly. Furthermore, we have restricted ourselves to simple one-dimensional geometries or networks composed of these. Of course a generalisation to two dimensions, e.g. as in [8, 12, 30, 52], is principally feasible. Considering a two-dimensional set-up, velocity density relations alone are not sufficient to provide a closure of the model but need to be combined with information on the direction. One option could be the use of the Eikonal equation with the velocity given by the velocity density relation used here, e.g. [19]. For other possibilities see e.g. [8, 12, 30, 52]. However, a comparison with the two-dimensional cellular automaton approach shows that in many cases a one-dimensional approach is sufficient.

For convenience, we have chosen a single microscopic model for the comparison of microscopic and macroscopic approaches to pedestrian flows. Nevertheless, the same results should also hold for most other microscopic pedestrian simulators. Although paths of individual pedestrians can differ significantly, the dynamics of the overall pedestrian density distribution are very similar among different microscopic approaches.

Acknowledgments. The authors would like to thank the German Federal Ministry of Education and Research who funded our research through the priority program Schutz und Rettung von Menschen within the project REPKA - Regional Evacuation: Planning, Control and Adaptation.

Appendix A. **Interpretation in terms of time-evolving measures.** Following the work of [12], a derivation of macroscopic pedestrian models can be obtained from a measure theory point of view. Taking a different view point allows us to systematically derive classical transport equations as a limit as well as a natural discretisation in terms of speed classes of the additional state variables.

Let μ_t be a positive Radon measure defined on the Borel σ-algebra $\mathcal{B}(\mathbb{R}) \otimes \mathcal{B}([0, V_{\max}])$ modelling pedestrian densities. For notational convenience we will consider $\mathcal{B}(\mathbb{R}) \otimes \mathcal{B}(\mathbb{R})$ and extend the measure outside $[0, V_{\max}]$ with zero. That is, for any $E \in \mathcal{B}(\mathbb{R}) \otimes \mathcal{B}(\mathbb{R})$ the number $\mu_t(E)$ gives the mass of pedestrians contained in E, i.e. pedestrians with a certain free flow velocity at a certain region. In contrast to kinetic models we work here with the free flow velocity rather than the actual velocity as used in models using phase-space variables. Following [9, 12] the balance of mass transported by a velocity field $v(v_{\text{ff}}, x, t) = v_{\text{ff}}\hat{v}(x, t)$ is expressed as

$$\frac{\partial \mu_t}{\partial t} + \frac{\partial}{\partial x}(\mu_t v) = 0 \quad \text{for } (v_{\text{ff}}, x, t) \in \mathbb{R} \times \mathbb{R} \times [0, T[\tag{6}$$

with $T > 0$ and along with some given initial distribution μ_0. All derivatives in (6) are interpreted in the functional sense of measures. The detailed relation v could be taken e.g. on the basis of Weidmanns fundamental relation, but any other relation would work as well, c.f. [12]. The formulation (6) is equivalent to the following weak formulation

$$\frac{d}{dt}\int_{\mathbb{R}}\int_{\mathbb{R}} \phi_x(x)\phi_x(v_{\text{ff}})d\mu_t(v_{\text{ff}}, x) = \int_{\mathbb{R}}\int_{\mathbb{R}} v(v_{\text{ff}}, x, t)\frac{\partial}{\partial x}\phi_x(x)\phi_v(v_{\text{ff}})d\mu_t(v_{\text{ff}}, x). \tag{7}$$

for all $\phi_x(\cdot), \phi_v(\cdot) \in \mathcal{C}_c^\infty(\mathbb{R})$. Under the assumption that the measure μ_t is absolutely continuous w.r.t. to the Lebesgue measure, Radon-Nikodym's theorem ensures the existence of a corresponding density, i.e. $d\mu_t = \rho(\cdot, t)d\mathcal{L}$ with $\rho(\cdot, t) \in \mathcal{L}$ and $\rho(\cdot, t) \geq 0$ almost everywhere. We thus obtain

$$\begin{aligned} &\frac{d}{dt}\int_{\mathbb{R}}\int_{\mathbb{R}} \rho(v_{\text{ff}}, x, t)\phi_x(x)\phi_v(v_{\text{ff}})dxdv_{\text{ff}} \\ &= \int_{\mathbb{R}}\int_{\mathbb{R}} \rho(v_{\text{ff}}, x, t,)v(v_{\text{ff}}, x, t))\frac{\partial}{\partial x}\phi_x(x)\phi_v(v_{\text{ff}})dxdv_{\text{ff}}. \end{aligned} \tag{8}$$

On the basis of this measure theoretic formulation, the classical model (1) as well as the corresponding numerical discretisation can be recovered as shown below.

Classical model. Considering only one single free flow velocity, i.e. $d\mu_t = \rho(x, t)\ \delta_{\tilde{v}_{\text{ff}}}d\mathcal{L}$, we recover

$$\frac{d}{dt}\int_{\mathbb{R}} \rho(\tilde{v}_{\text{ff}}, x, t)\phi_x(x)dx = \int_{\mathbb{R}} \rho(\tilde{v}_{\text{ff}}, x, t)v(\tilde{v}_{\text{ff}}, x, t)\frac{\partial}{\partial x}\phi_x(x)dx. \tag{9}$$

The equivalent strong formulation is the classical model (1).

Numerical discretisation. For simulations of model (5) a corresponding discretisation of the space as well as the free flow velocities is required. With respect to the velocity space, we adopt a classical Galerkin approximation. Since $\rho(v_{\text{ff}}, x, t) \in \mathcal{L}$, we can choose the following representation with respect to the infinite dimensional basis $\psi_i(v)$ of the velocity space

$$\rho(v_{\text{ff}}, x, t) = \sum_{i=0}^{\infty} \rho_i(x, t)\psi_i(v_{\text{ff}}). \tag{10}$$

Introducing a discretisation of the velocity space $0 = v_0 < v_1 < \ldots < v_n = V_{\max}$, a corresponding finite n-dimensional basis is given by the piecewise constant orthonormal functions $\psi_i(v) = \frac{1}{\sqrt{v_i - v_{i-1}}}\chi_{[v_{i-1}, v_i]}(v)$. The densities ρ_i can be interpreted as densities corresponding to a certain velocity class, namely pedestrians with a free

flow velocity between v_{i-1} and v_i. Adopting this finite dimensional basis and using $v(v_{\text{ff}}, x, t)) = v_{\text{ff}}\hat{v}(x,t)$, (8) reduces to

$$\begin{aligned}&\sum_j \frac{d}{dt}\int_{\mathbb{R}}\int_{\mathbb{R}} \rho_j(x,t)\psi_j(v_{\text{ff}})\phi_x(x)\phi_v(v_{\text{ff}})dxdv_{\text{ff}}\\ &= \sum_j \int_{\mathbb{R}}\int_{\mathbb{R}} \rho_j(x,t)\psi_j(v_{\text{ff}})v_{\text{ff}}\hat{v}(x,t)\frac{\partial}{\partial x}\phi_x(x)\phi_v(v_{\text{ff}})dxdv_{\text{ff}}\end{aligned} \tag{11}$$

for all ψ_i. Using the fact that we work with an orthonormal basis we obtain

$$\frac{d}{dt}\int_{\mathbb{R}} \rho_j(x,t)\phi(x)dxdv_{\text{ff}} = \sum_j \int_{\mathbb{R}} \rho_j(x,t)\bar{v}_{\text{ff}}\hat{v}(x,t)\frac{\partial}{\partial x}\phi(x)dx \tag{12}$$

for all $\bar{v}_{\text{ff}}$. Here, we use the notation that the index $\bar{v}_{\text{ff}}$ corresponds to the index i with average velocity $\bar{v}_{\text{ff}} = \int_{\mathbb{R}} v_{\text{ff}}\psi_i\psi_i = (v_i - v_{i-1})/2$. Thus we have recovered separate evolution equations for each velocity class (in total n).

Since the strong formulation of(12) corresponds more or less classical structure (1), they can easily be discretised using the concepts introduced in Appendix B.

Appendix B. **Numerical discretisation.** Simulations of the balance equation (1) in one dimension are typically based on finite volume schemes. Considering first order approximations typically upwind schemes are used [38]. However, since these classical schemes rely solely on upwind information, in case of congestions (e.g. the example of a narrowing street presented in Section 4.1) they could lead to densities higher than $\rho_{\max}$. Thus the evident assumption of an existence of a maximal density (c.f. e.g. [51]) is violated. Therefore, we shall introduce a non-standard mixed upwind-downwind scheme for the simulation of pedestrian flows. Here, we shall restrict ourselves to a PDE on a single street. Following [10] corresponding discretisations can be mapped on a network of streets (c.f. Section 2.1).

For simplicity, let us consider in the following a street of constant width with a directed flow of pedestrians (an assumption typically valid in an evacuation). Furthermore, we assume that space and time are discretised equidistantly, i.e. x_0, x_1, …, x_n such that $x_i - x_{i-1} = \Delta_x$ and t^0, t^1, …, t^m such that $t^j - t^{j-1} = \Delta_t$. Let ρ_i^j be a piecewise (cell wise) constant approximation of the density at position x_i at time t^j, i.e. $\rho_i^j = \rho(x_i, t^j)$. Adopting a first order discretisation we rely on the following scheme

$$\rho_i^{j+1} = \rho_i^j - \Delta_t\left[d^+F_\Delta^+ + d^-F_\Delta^-\right] \tag{13}$$

with the discretised fluxes

$$\begin{aligned}F_\Delta^+ &= \frac{\rho_i v((1-\alpha)\rho_i + \alpha\rho_{i+1}) - \rho_{i-1}v((1-\alpha)\rho_{i-1} + \alpha\rho_i)}{\Delta_x}\\ F_\Delta^- &= \frac{\rho_{i+1} v((1-\alpha)\rho_{i+1} + \alpha\rho_i) - \rho_i v((1-\alpha)\rho_i + \alpha\rho_{i-1})}{\Delta_x}\end{aligned}$$

and direction indicators

$$d^+ = \begin{cases}0 & v \geq 0\ (\rightarrow)\\ 1 & v < 0\ (\leftarrow)\end{cases} \qquad d^- = \begin{cases}0 & v \geq 0\ (\rightarrow)\\ 1 & v < 0\ (\leftarrow)\end{cases}$$

(the direction of movement is indicated by arrows). In the case v = const., the scheme is a classical first order upwind scheme [38]. Considering a non-constant v, e.g. as given by (3), the scheme (13) differs from classical upwind schemes by the

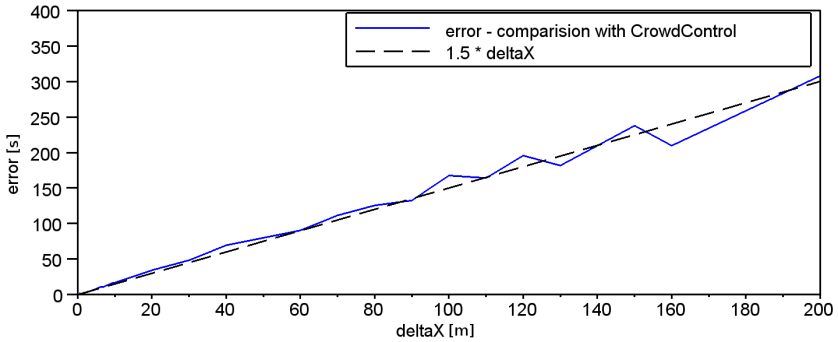

FIGURE 12. Error in evacuation time of 80% of 2000 pedestrians in a street of length 200m and width 10m, where the exact solution has been determined using a discretisation of Δ_x =0.1m.

introduction of the parameter $0 \leq \alpha \leq 1$. Choosing $\alpha = 0$ the scheme is a classical first order upwind scheme. Choosing $\alpha = 1$, i.e. evaluating densities / velocities downwind, the scheme mimics central properties of the balance equation (1) in combination with a fundamental diagram like (3). On the one hand, the scheme is conservative by construction. On the other hand it guarantees that ρ is always bounded by $\rho_{\max}$ as required by (3) or any other fundamental diagram. Above a certain density $\rho_{\max}$ pedestrians cannot move any more and thus the density cannot increase further. In the following we shall always set $\alpha = 1$ to guarantee boundedness of densities by $\rho_{\max}$.

The parameter α also allows for a different interpretation, namely the measure of how far pedestrians look ahead to adjust their velocity according to the density. In case of a relatively fine discretisation $\Delta_x = 1m$ $\alpha = 1$ would imply that pedestrians look roughly 1m ahead to adjust their velocities and in the case of a coarse discretisation $\Delta_x = 10m$ $\alpha = 0$ would imply that pedestrians look less than 10m ahead to adjust velocities.

The spatial discretisation Δ_x is chosen manually according to the required accuracy (c.f. also Figure 12). The temporal discretisation Δ_t is then chosen automatically accordingly to the CFL condition [38], i.e. $\Delta_t = 0.1v/\Delta_x$. In Figure 12 a detailed convergence study with respect to evacuation times is shown. Here, we consider a street of length 200m and width 10m with 2000 pedestrians and determine the evacuation of 80% of the pedestrians. Errors for different spatial discretisation levels are shown, where the exact solution has been determined with the solution of the microscopic model. The same relationship for the error is found using a very small Δ_x to determine the exact solution. One can clearly observe the discretisation is of first order as expected (c.f. also the experimental order of convergence determined in Table 3).

Appendix C. **Efficient microscopic discrete-in-time model.** The structured hyperbolic macroscopic model outlined in Section 3, shows significantly more realistic dynamics than classical macroscopic models and is still significantly faster to solve than exact microscopic models. In this Appendix, we shall further introduce an alternative simple one-dimensional microscopic discrete-in-time model aimed at

Δ_x	0.5m	1m	5m	10m	50m	100m
Error E	0s	2.1s	10.2s	18.9s	82.0s	169.7s
EOC	0	0.9	0.85	1.03	0.61	2.19

TABLE 3. Experimental order of convergence (EOC= $(\ln E^i - \ln E^{i+1})/(\ln \Delta_x^i - \ln \Delta_x^{i+1})$) with respect to evacuation of 80% of 2000 pedestrians in a street of length 200m and width 10m, where the exact solution has been determined using a discretisation of Δ_x =0.1m.

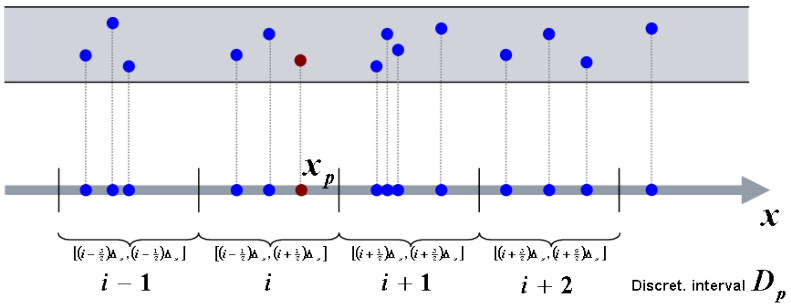

FIGURE 13. Schematic sketch of the projected dynamics scheme: each pedestrian is characterised by its one-dimensional position x_p and the discretisation interval D_p corresponding to its position. Pedestrian densities ρ are discretised piecewise constantly on the discretisation intervals.

faster computations with the requirement that it reproduces exactly the dynamics of the microscopic model presented in Section 2.2. It is as realistic and computationally efficient as the structured macroscopic model. Again we restrict ourselves to a single street, but a generalisation to networks is straightforward because of the microscopic nature of the model.

The central idea of this simple multiscale approach is to couple a microscopic model projected to one dimension with a macroscopic estimation of pedestrian densities using a proper macroscopic discretisation (piecewise constant). These macroscopic estimates are then used to determine the velocities of microscopic pedestrians via fundamental relations, e.g. (3). The proposed approach is shown schematically in Figure 13.

The one-dimensional representation of the street is discretised into discrete intervals and each pedestrian p is characterised by a position x_p and the discrete interval D_p the pedestrian resides in. Adopting a temporal discretisation with time steps Δ_t, in each time step all pedestrians are moved according to Algorithm 1. First, the velocity of each pedestrian V_p is evaluated on the basis of the actual position x_p and the density of pedestrians in the current discretisation interval D_p and the next discretisation interval D_{p+1} in the direction of movement. Second, the detailed weight is chosen by a parameter α , i.e. $\hat{\rho} = (1-\alpha)\rho(D_p) + \alpha\rho(D_{p+1})$ is used to determine corresponding velocities, where $\rho(D_p)$ is the density in the interval D_p given by the number of pedestrians on that interval divided by the corresponding area. The interpretation of α is analogous to Appendix B. Again $\alpha = 1$ ensures a

maximal density of $\rho_{\max}$. The speed V_p is then given by a fundamental diagram, e.g. $v(v_{\text{ff}};\hat{\rho}) = v_{\text{ff}}(1 - exp(-\gamma(1/\hat{\rho} - 1/\rho_{\max})))$ as given by relation (3) and v_{ff} varying among pedestrians. In the next step, the position of the pedestrian is updated according to $x_p + V_p\Delta_t$. If this position would be in the next discretisation interval, i.e. $x_p + V_p\Delta_t > D_{p+1}$, the pedestrian is moved to the beginning of the next discretisation interval and the movement step is repeated for the remaining time. Otherwise, the pedestrian is simply moved to the new position in the same interval and the algorithm proceeds with the next pedestrian.

Algorithm 1 Projected dynamics scheme - update pedestrian p in interval D_p with free flow velocity v_{ff}^p and position x_p in a time step of length Δ_t.

initialise time to move $\delta_p = \Delta_t$
while $\delta_p > 0$ **do**
  determine density $\hat{\rho} = (1-\alpha)\rho(D_p) + \alpha\rho(D_{p+1})$
  determine velocity $V_p = v_{\text{ff}}(1 - exp(-\gamma(1/\hat{\rho} - 1/\rho_{\max})))$
  determine distance $d_p = V_P\Delta_t$
  if $x_p + d_p \leq (D_p + \frac{1}{2})\Delta_x$ **then**
    $x_p = x_p + d_p$
    $\delta_p = 0$
  else
    $\delta_p = \delta_p - ((D_p + \frac{1}{2})\Delta_x - x_p)/(V_p)$
    $x_p = (D_p + \frac{1}{2})\Delta_x$
  end if
end while

A comparison of this new multiscale algorithm with the detailed microscopic model (Section 2.2) and the newly introduced structured macroscopic model (Section 3) is shown in Figure 14 for the simple scenario outlined in Section 2.3. We find that qualitatively the model reproduces the microscopic models as well as the structured macroscopic model. Considering different macroscopic discretisations analogous to the structured macroscopic model (c.f. Figure 12), we also recover a linear relationship for the discretisation error (Figure 15). That is, the newly introduced simple multiscale model is a first order approximation, as expected. Compared with classical microscopic approaches this multiscale approach shows a significant computational speed up. It is as efficient as the structured macroscopic model introduced in Section 3 and dynamics are of the same realism. Thus it is a proper alternative.

REFERENCES

[1] C. Appert-Rolland, P. Degond and S. Motsch, Two-way multi-lane traffic model for pedestrians in corridors, *Netw. Heterog. Media*, **6** (2011), 351–381.
[2] N. Bellomo and A. Bellouquid, On the modeling of crowd dynamics: Looking at the beautiful shapes of swarms, *Netw. Heterog. Media*, **6** (2011), 383–399.
[3] N. Bellomo and V. Coscia, First order models and closure of the mass conservation equation in the mathematical theory of vehicular traffic flow, *CR Mecanique*, **333** (2005), 843–851.
[4] N. Bellomo and C. Dogbe, On the modeling of traffic and crowds: a survey of models, speculations, and perspectives, *SIAM* Rev., **53** (2011), 409–463.
[5] N. Bellomo, M. Delitala and V. Coscia, On the mathematical theory of vehicular traffic flow I: Fluid dynamic and kinetic modelling, *Math. Mod. Meth. Appl. S.*, **12** (2002), 1801–1843.
[6] V. Blue, M. Embrechts and J. Adler, Cellular automata modeling of pedestrian movements, *IEEE Int. Conf. on Syst., Man and Cybern.*, (1997), 2320.

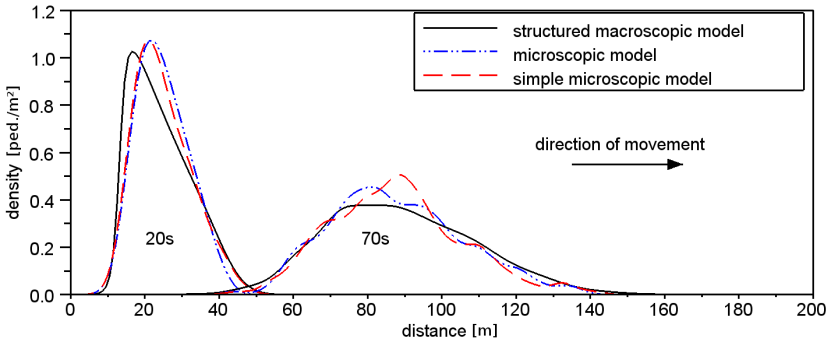

FIGURE 14. Comparison of a structured macroscopic model (using a finite volume scheme with $\Delta_x = 1$m for simulations), an individual based microscopic model and the new simple multiscale model for a pedestrian flow in a street (length = 200m, width = 10m, persons = 200) moving from the left to the right. Snapshots at two different time-steps (20s, 70s) are shown.

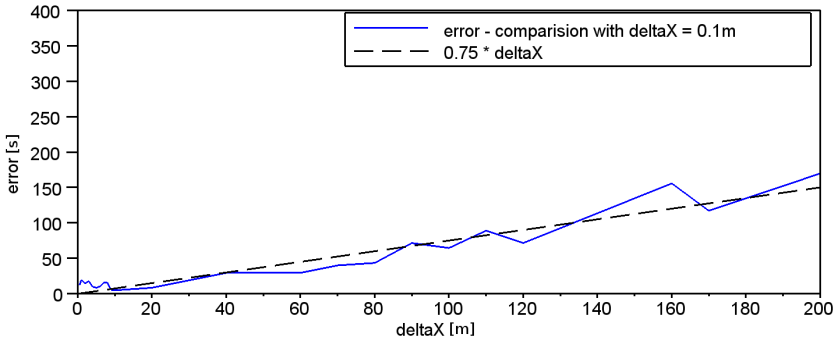

FIGURE 15. Error in evacuation time of 80% of 2000 pedestrians in a street of length 200m and width 10m, where the exact solution has been determined with the structured macroscopic model using a discretisation of Δ_x =0.1m.

[7] C. Burstedde, K. Klauck, A. Schadschneider and J. Zittartz, Simulation of pedestrian dynamics using a two-dimensional cellular automaton, *Physica A*, **295** (2001), 507–525, arXiv:cond-mat/0102397.

[8] V. Coscia and C. Canavesio, First-order macroscopic modelling of human crowd dynamics, *Math. Mod. Meth. Appl. S.*, **18** (2008), 1217–1247.

[9] C. Canuto, F. Fagnani and P. Tilli, A eulerian approach to the analysis of rendez-vous algorithms, *Proceedings of the 17th IFAC World Congress*, (2008), 9039–9044.

[10] G. M. Coclite, M. Garavello and B. Piccoli, Traffic flow on a road network, *SIAM J. Appl. Math.*, **36** (2005), 1862–1886.

[11] M. Chraibi, U. Kemloh, A. Schadschneider and A. Seyfried, Force-based models of pedestrian dynamics, *Netw. Heterog. Media*, **6** (2011), 425–442.

[12] E. Christiani, B. Piccoli and A. Tosin, Multiscale modeling of granular flows with applications to crowd dynamics, *Multiscale Model. Sim.*, **9** (2011), 155–182.

[13] R. M. Colombo and M. D. Rosini, Pedestrian flows and nonclassical shocks, *Mathematical Methods in the Applied Sciences*, **28** (2005), 1553–1567.
[14] M. Chraibi, A. Seyfried and A. Schadschneider, Generalized centrifugal force model for pedestrian dynamics, *Phys. Rev. E*, **82** (2010), 046111.
[15] C. F. Daganzo, *Fundamentals of Transportation and Traffic Operations*, Pergamon, Oxford, 1997.
[16] M. Fukui and Y. Ishibashi, Self-organized phase transitions in cellular automaton models for pedestrians, *J. Phys. Soc. Jap.*, **68** (1999), 2861.
[17] S. Göttlich, M. Herty and A. Klar, Network models for supply chains, *Commun. Math. Sci.*, **3** (2005), 545–559.
[18] S. Göttlich, S. Kühn, J. Ohst, S. Ruzika and M. Thiemann, Evacuation dynamics influenced by spreading hazardous material, *Netw. Heterog. Media*, **6** (2011), 443–464.
[19] D. Hartmann, Adaptive pedestrian dynamics based on geodesics, *New J. Phys.*, **12** (2010), 043032.
[20] D. Helbing, A fluid-dynamic model for the movement of pedestrians, *Complex Systems*, **6** (1992), 391–415.
[21] L. F. Henderson, On the fluid mechanics of human crowd motion, *Transport. Res.*, **8** (1974), 509–515.
[22] H.-J. Huang and R.-Y. Guo, Static floor field and exit choice for pedestrian evacuation in rooms with internal obstacles and multiple exits, *Phys. Rev. E.*, **78** (2008), 021131.
[23] D. Helbing and A. Johansson, Pedestrian, crowd and evacuation dynamics, *Encyclopedia of Complexity and Systems Science*, **16** (2010), 6476–6495.
[24] M. Herty and A. Klar, Modeling, simulation, and optimization of traffic flow networks, *SIAM J. Sci. Comput.*, **25** (2003), 1066–1087.
[25] D. Helbing and P. Molnár, Social Force Model for Pedestrian Dynamics, *Phys. Rev. E*, **51** (1995), 4282–4286.
[26] H. Holden and N.H. Risebro, A mathematical model of traffic flow on a network of unidirectional roads, *SIAM J. Math. Anal.*, **26** (1995), 999–1017.
[27] H. W. Hamacher and S. A. Tjandra, *Mathematical modelling of evacuation problems: A state of the art*, in *Pedestrian and Evacuation Dynamics* (eds. M. Schreckenberg and S. D. Sharma), Springer, 2002, 227–266.
[28] R. L. Hughes, A continuum theory for the flow of pedestrians, *Transport. Res. B - Meth.*, **36** (2002), 507–535.
[29] R. L. Hughes, The flow of human crowds, *Annu. Rev. Fluid Mech.*, **35** (2003), 169–182.
[30] L. Huang, S. C. Wong, M. Zhang, C.-W. Shu and W. H. K. Lam, Revisiting Hughes' dynamic continuum model for pedestrian flow and the development of an efficient solution algorithm, *Transport. Res. B - Meth.*, **43** (2009), 127–141.
[31] P. Kachroo, S. J. Al-Nasur, S. A. Wadoo and A. Shende, *Pedestrian Dynamics - Feedback Control of Crowd Evacuation*, Springer, New York, 2008.
[32] B. S. Kerner, *The Physics of Traffic*, Springer, New York, 2004.
[33] G. Köster, D. Hartmann, and W. Klein, Microscopic pedestrian simulations: From passenger exchange times to regional evacuation, in *Operations Research Proceedings* (eds. B. Hum, K. Morasch, S. Pickl and M. Siegle), Springer, 2010, 571–576.
[34] H. Klüpfel, *A Cellular Automaton Model for Crowd Movement and Egress Simulation*, Ph.D. thesis, Universität Duisburg-Essen in Duisburg, 2003.
[35] A. Kneidl, M. Thiemann, A. Borrmann, S. Ruzika, H. W. Hamacher, G. Köster and E. Rank, Bidirectional Coupling of Macroscopic an Microscopic Approaches for Pedestrian Behavior Prediction, in *Pedestrian and Evacuation Dynamics* (eds. R. D. Peacock, E. D. Kuligowski and J. D. Averill), Springer, 2011, 459–470 .
[36] A. Kneidl, M. Thiemann, D. Hartmann and A. Borrmann, *Combining pedestrian simulation with a network flow optimization to support security staff in handling an evacuation of a soccer stadium*, in *Proceedings of European Conference Forum 2011* (eds. E. Tobin and M. Otreba), University College Cork, Cork, 2011.
[37] R. Löhner, On the modeling of pedestrian motion, *Appl. Math. Model.*, **34** (2010), 366–382.
[38] R. J. LeVeque, *Numerical Methods for Conservation Laws*, Birkhäuser, Basel, 2005.
[39] T. I. Lakoba, D. J. Kaup and N. M. Finkelstein, Modifications of the Helbing-Molnár-Farkas-Vicsek social force model for pedestrian evolution, *Simulation*, **81** (2005), 339–352.
[40] K. Nishinari, A. Kirchner, A. Namazi and A. Schadschneider, Extended floor field CA model for evacuation dynamics, *IEICE Trans. Inf. Syst.*, **E87D** (2004), 726–732.

[41] M. Oppenhäuser, *Realisierung und Potenzialanalyse von wissenschaftlichen Konzepten zur Regionalen Evakuierung aus Polizeilicher Sicht am Beispiel des Projektes REPKA*, Master's Thesis, German Police University, Münster, 2011, http://opac.pfa-ms.de/onlinedokumente/masterarbeiten/2011/Oppenhaeuser_Markus.pdf.
[42] N. Pelechano, J. M. Allbeck and N. Badler, *Virtual Crowds: Methods, Simulation, and Control*, Morgan & Claypool Publishers, San Rafael, Calif., 2008.
[43] D. R. Parisi, M. Gilman and H. Moldovan, A modification of the social force model can reproduce experimental data of pedestrian flows in normal conditions, *Physica A*, **388** (2009), 3600–3608.
[44] I. Prigogine and R. Herman, *Kinetic Theory of Vehicular Flow*, Elsevier, New York, 1971.
[45] W. H. Press, S. A. Teukolsky, W. T. Vetterling and B. P. Flannery, *Numerical Recipes: The Art of Scientific Computing*, Cambridge University Press, New York, 2007.
[46] *REPKA, Regionale Evakuierung: Planung, Kontrolle und Anpassung*, http://www.repka-evakuierung.de/.
[47] E. V. RiMEA, *Richtlinie für Mikroskopische Entfluchtungsanalysen*, http://www.rimea.de/.
[48] A. Schadschneider, W. Klingsch, H. Klüpfel, T. Kretz, C. Rogsch and A. Seyfried, Evacuation dynamics: Empirical results, modeling and applications, *Encyclopedia of Complexity and System Science*, (2009), 3142–3176.
[49] A. Schadschneider and A. Seyfried, Empirical results for pedestrian dynamics and their implications for modeling, *Netw. Heterog. Media*, **6** (2011), 545–560.
[50] A. Varas, M. D. Cornejo, D. Mainemer, B. Toledo, J. Rogan, V. Munoz and J. A. Valdivia, Cellular automaton model for evacuation process with obstacles, *Physica A*, **382** (2007), 631–642.
[51] U. Weidmann, *Transporttechnik der Fussgänger: Transporttechnische Eigenschaften des Fussgängerverkehrs (Literaturauswertung)* Schriftenreihe des IVT, University of Zurich in Zurich, 1993.
[52] Y. Xia, S. C. Wong and C. W. Shu, Dynamic continuum pedestrian flow model with memory effect, *Phys. Rev. E*, **79** (2009), 066113.
[53] W. J. Yu, R. Chen, L. Y. Dong and S. Q. Dai, Centrifugal force model for pedestrian dynamics, *Phys. Rev. E*, **72** (2005), 026112.
[54] K. Yamamoto, S. Kokubo and K. Nishinari, Simulation for pedestrian dynamics by real-coded cellular automata, *Physica A*, **379** (2007), 654.

Received August 2012; revised April 2013.

E-mail address: hartmann.dirk@siemens.com
E-mail address: isabella.vonsivers@googlemail.com